

OPEN ACCESS

Self-Assembly of Symmetric GaAs Quantum Dots on (111)A Substrates: Suppression of Fine-Structure Splitting

To cite this article: Takaaki Mano *et al* 2010 *Appl. Phys. Express* **3** 065203

View the [article online](#) for updates and enhancements.

You may also like

- [Reducing “slice cross-talk” effect in metamaterial assisted fast spin-echo MRI](#)
E Brui, S Rapacchi, D Bendahan *et al.*
- [Spectroscopic Studies of Cation Structure Dependence on Lithium-Ion Conductivity in Phosphonium Ionic Liquid Electrolytes](#)
Shoki Nawate, Abbas Alshehabi, Mitsuhiro Matsumoto *et al.*
- [Comparative study between conventional and mechanical technology on fecal sludge treatment plants \(FSTP\) in Indonesia](#)
A M Stevani and P Soewondo



The Electrochemical Society
Advancing solid state & electrochemical science & technology



249th
ECS Meeting
May 24-28, 2026
Seattle, WA, US
Washington State
Convention Center

Spotlight Your Science

**Submission deadline:
December 5, 2025**

SUBMIT YOUR ABSTRACT

Self-Assembly of Symmetric GaAs Quantum Dots on (111)A Substrates: Suppression of Fine-Structure Splitting

Takaaki Mano, Marco Abbarchi, Takashi Kuroda, Brian McSkimming, Akihiro Ohtake, Kazutaka Mitsuishi, and Kazuaki Sakoda

National Institute for Materials Science, 1-2-1 Sengen, Tsukuba, Ibaraki 305-0047, Japan

Received March 24, 2010; accepted May 6, 2010; published online May 28, 2010

Great suppression of fine-structure splitting (FSS) is demonstrated in self-assembled GaAs quantum dots (QDs) grown on AlGaAs(111)A surface. Due to the three-fold rotational symmetry of the growth plane, highly symmetric excitons with significantly reduced FSS are achieved. Scanning tunneling microscopy and cross-sectional transmission microscopy demonstrate a laterally symmetric dot shape with abrupt interface. Polarized photoluminescence spectra confirm excitonic transition with FSS smaller than $\sim 20 \mu\text{eV}$, a substantial reduction from that of QDs grown on (100).
© 2010 The Japan Society of Applied Physics

DOI: 10.1143/APEX.3.065203

Semiconductor quantum dots (QDs) are attracting much interest because of their potential application in entangled photon sources, which would serve as a key unit for quantum information technology. The generation of entangled photons in the QDs relies on the twin-photon emission associated with the transition cascade from the biexciton state to the exciton state, and to the ground state. Thanks to the spinor nature of excitons, this transition path becomes two-fold. When these two paths are indistinguishable, the two photons become entangled on a polarization basis.¹⁾

Many studies have focused on Stranski–Krastanov (SK) growth of QDs on (100) surfaces. However, these QDs normally exhibit significant fine-structure splitting (FSS) due to the elongated morphology, strain-induced piezoelectric field, and intermixing between InAs and GaAs.²⁾ Several approaches have been reported for solving these problems, such as high-temperature annealing³⁾ and the application of external fields.^{4–6)} In the first case, however, only small percentage of total QDs exhibited small FSS. The latter approach requires a complicated setup, which is not practical. It is therefore desirable to establish an alternative technique for the self-assembly of symmetric QDs.

Very recently, the reduction of FSS using (111) surface was predicted theoretically,^{7,8)} and demonstrated experimentally.^{9,10)} Note that, via SK growth, it is difficult to obtain QDs on the (111) substrates. Thus, they used patterned substrates (inverted pyramids)⁹⁾ or droplet epitaxy (DE),¹⁰⁾ both producing InGaAs QDs on GaAs(111)B. In the former case, however, highly complex processes, such as electron beam lithography, are required for preparing the patterned substrates. Also, a large number of impurities might be incorporated during these processes, which would shorten the carrier lifetime. In the latter case, they applied DE to the lattice-mismatched system, implying the lowering of morphological quality compared to the lattice-matched case.¹¹⁾

In this study, we demonstrate the self-assembly of GaAs QDs on AlGaAs(111)A surfaces via DE.^{12–14)} In the case of DE in the lattice-matched GaAs/AlGaAs system, the formation of strain-free, nearly pure GaAs QDs was realized. Owing to the three-fold rotational symmetry of the growth plane, well-defined, highly symmetric QDs were formed. Moreover, excitons with significantly reduced FSS were achieved in all the investigated QDs.

The sample was grown using a conventional molecular beam epitaxy system. After the growth of a GaAs buffer and AlGaAs barrier layer on the GaAs(111)A substrate at 500 °C, followed by annealing at 600 °C, Ga droplets were formed by supplying a 0.45 monolayer (ML) of Ga (0.09 ML/s) at 350 °C. Then, the substrate was cooled down to 200 °C, and crystallized into GaAs by supplying an As₄ flux of 2×10^{-6} Torr beam equivalent pressure. The sample was then annealed at 400 °C (or 500 °C), followed by capping with an Al_{0.3}Ga_{0.7}As layer. Finally, rapid thermal annealing was performed to improve the optical properties (800 °C for 4 min).

The structural properties were studied by *in vacuo* scanning tunneling microscopy (STM),¹⁵⁾ and atomic force microscopy (AFM) in an ambient environment. The QDs embedded in AlGaAs were further studied by cross-sectional high angle annular dark field scanning transmission electron microscopy (HAADF-STEM). Optical properties were analyzed by low-temperature photoluminescence (PL) measurement based on both ensemble and micro objectives. A continuous wave laser emitting at 532 nm was used for excitation. Excitation polarization was set to be linear to avoid the Overhauser effect.¹⁶⁾ μPL experiments were performed using a confocal setup with lateral resolution of about 1 μm . The collected PL was dispersed by polychromator and detected by charge coupled device (CCD) camera with spectral resolution of 130 μeV .

Figure 1(a) shows an AFM image of bare GaAs QDs before capping. Well-defined QDs are present with a spatial density of $2.5 \times 10^{10} \text{ cm}^{-2}$. They exhibit a disk-like shape with a base diameter of 38 nm and a height of 1.0 nm on average. The base size shows a rather uniform distribution (17%), while the height is highly distributed (56%). This fact suggests that carrier quantization and its energy distribution are governed by vertical confinement along the growth direction.

Figure 1(b) summarizes the cross-sectional AFM profiles of three QDs differing in size. For each QD, the cross sections along two orthogonal directions ([211] and [01 $\bar{1}$]) are of identical shape. Such isotropic feature is in stark contrast to QDs previously grown on the (100) surface; those were elongated by 5–20% along the [110] direction.¹⁴⁾ Thus, QD symmetry was substantially improved by using the (111)A substrate.



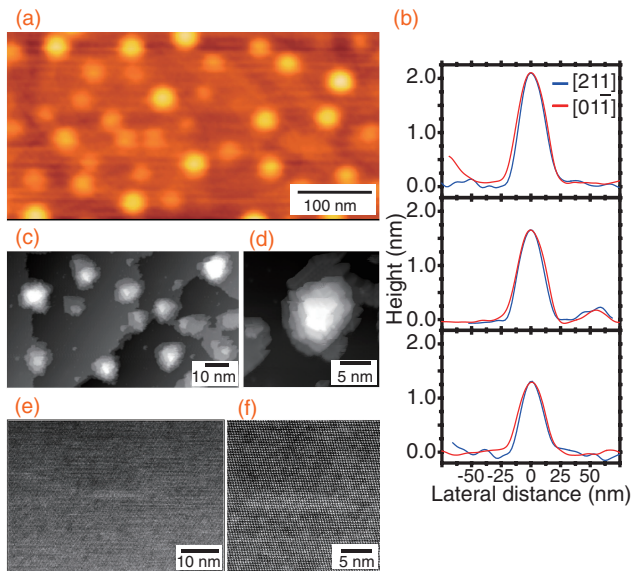


Fig. 1. (a) AFM image of GaAs QDs formed on AlGaAs(111)A surface. The surface QDs were annealed at 400 °C for 10 min. Scan area is 250 × 500 nm². (b) Cross-sectional AFM profiles of three QDs differing in size along the [211] and [011] directions. (c, d) *In vacuo* STM images of GaAs QDs formed on GaAs(111)A surface. (e, f) Cross-sectional HAADF-STEM images of GaAs QD [shown in (a)] capped with AlGaAs.

Note that in the DE growth, Ga droplets have circular symmetry independent of their bottom surface due to the loss of bonding at the liquid-solid interface. Elongation must take place at the crystallization and annealing stages, where the final QD shape is determined by the complex interplay between Ga flow (from droplets) and As flow (from As₄ flux), which is quite sensitive to the surface anisotropy. For the (111)A plane, on the other hand, equivalent directions appear with respect to every 120° rotation, thus removing in-plane anisotropy in an ideal case.

Figures 1(c) and 1(d) show *in vacuo* STM images of GaAs QDs. Again, elongation is not evidenced, but random orientation is exhibited, which reflects the microscopic environment at the surface. Such orientation randomness might have been emphasized by the formation of an atomic step/terrace structure at the side surface, rather than the formation of preferential facets. The morphology is nearly truncated pyramid with an atomically-flat top.

Figures 1(e) and 1(f) present cross-sectional STEM images of a GaAs QD embedded in AlGaAs. A buried QD with truncated shape is again visible. The presence of a clear interface suggests an abrupt boundary between the matrix and QDs, free from intermixing. There is no indication of defects, supporting high crystal quality. We also note the absence of a two-dimensional GaAs wetting layer underneath the QDs. This is consistent with the present growth conditions where the nominal amount of Ga deposition was 0.45 ML, much less than 1 ML.

Figure 2 shows a low-temperature PL spectrum of the ensemble of GaAs QDs. High-yield PL was observed at a wavelength of 720 nm (1.72 eV) with 180 meV FWHM. The PL spectrum consists of multiple peaks, rather than a broad band. Such spectral signature was independent of excitation intensity (not shown) and thus not ascribed to the state-

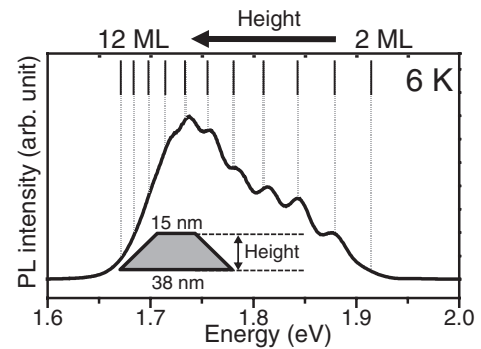


Fig. 2. PL spectrum of the ensemble of GaAs QDs, measured at 6 K. The vertical lines show the calculated energy levels, assuming a truncated cone shape with constant top (15 nm) and bottom (38 nm) diameters.

filling of QD levels. We attribute the spectral multiplet to ground state emissions from different GaAs QD families whose heights vary by a ML step, reflecting a flat shape with atomically-smoothed top, as was proven in Figs. 1(c) and 1(e). The vertical lines plotted in Fig. 2 represent the transition energies calculated within the framework of the effective mass model.¹⁷⁾ In this calculation we assumed a truncated cone shape with constant top and bottom diameters (15 and 38 nm, respectively, as deduced by AFM analysis), and changed the height by a ML step (0.32 nm). As shown in Fig. 2, this model perfectly reproduces the spectral multiplets, thus, confirming the validity of our model.

Figure 3(a) shows an example of a μ PL spectrum in the (111)A GaAs QDs.¹⁸⁾ It consists of several sharp peaks, for which the linewidth, limited by the resolution of our equipment, is less than 50 μ eV. Figure 3(b) displays the dependence of the energy of two representative lines, which are denoted by X and T in Fig. 3(a), as a function of the angle of analyzer polarization. By fitting the data with a sinusoidal dependence we extract the amplitude of the oscillation (which represents the FSS) and its phase (the PL polarization axis). It was found that X showed a significant polarization-dependent shift having an amplitude of 27 μ eV, while T did not exhibit a shift. The observation of sinusoidal dependence naturally led us to attribute X to a neutral exciton that gave rise to anisotropic FSS, and T to a trion. Note that all PL lines were categorized as either of two groups, one with polarization dependence (like X), and the other without (like T), allowing FSS statistics to be characterized.

Figure 3(c) presents a comparison between the absolute value of the FSS [as determined by the analysis shown in Fig. 3(b)] in GaAs(111)A QDs and that in (100) QDs reported as a function of the corresponding X emission energy. The latter series was previously reported.^{14,19,20)} For (111)A, the magnitude of FSS was 17 μ eV on average. Note that this value must be overestimated, because QDs with FSS smaller than the fit accuracy (\sim 10 μ eV) were not included in our statistical analysis, even though, the magnitude of FSS in (111)A was much smaller than that of (100), for which the average was 54 μ eV. This is the direct consequence of the improved symmetry of QDs grown on (111)A with respect to the (100) case.

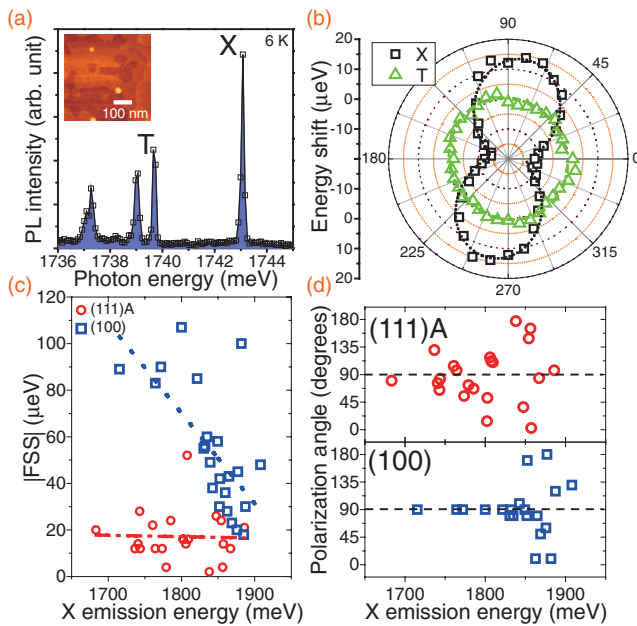


Fig. 3. (a) Typical PL spectrum of a single GaAs QD at 6 K. (b) PL energy shift as a function of the detected polarization angle for X (squares in black) and T (triangles in green) of the QD shown in (a). The dotted black (green) line is a sinusoidal fit to X (T) energy shift. (c) Summary of the FSS of QDs grown on (100) (squares in blue) and on (111)A (circles in red). The lines are guides for the eye. (d) Top (bottom) panel displays the polarization axes of the QDs grown on the (111)A [(100)] surface as a function of X emission energy (90° corresponds to the $[211]$ [$1\bar{1}0$] in-plane direction). The inset of (a) shows an AFM image of low-density GaAs QDs used for the μPL study.

Figure 3(d) shows the dependence of the linear polarization axis, which was determined by the polar plot analysis [Fig. 3(b)], as a function of X emission energy. The (111)A QDs showed completely disordered behavior of the polarization axis, confirming the absence of preferential in-plane directions. On the other hand, in the (100) QDs the polarization axis was mostly aligned along the $[1\bar{1}0]$ direction, while it became randomly oriented for energies higher than 1.8 eV. The elongation of QDs on (100) was enhanced for larger dots, which suffered more from anisotropic atomic diffusion during growth.¹⁴ Thus, even for (100), sufficiently small QDs would possibly give negligible FSS, which has been confirmed in In(Ga)As/GaAs QDs grown via the SK method.⁵ In contrast, (111)A QDs present the complete absence of preferential polarization axes, suggesting a much higher probability of finding QDs with zero FSS in a wide range of wavelengths. Such characteristics are highly favorable for QDs application to entangled photon sources.

In conclusion, we demonstrated highly symmetric and strain-free GaAs QDs grown on a (111)A substrate. The absence of elongation and that of the facet formation were confirmed by morphological analysis. FSS was substantially reduced in comparison with the QDs grown on (100). We believe that the present system assured the removal of every macroscopic origin that induced QD asymmetry, while residual FSS due to microscopic randomness could be removed by post-selection procedures.

Acknowledgment This work was partially supported by a Grant-in-Aid for Scientific Research from the Ministry of Education, Culture, Sports, Science and Technology of Japan.

- 1) O. Benson, C. Santori, M. Pelton, and Y. Yamamoto: *Phys. Rev. Lett.* **84** (2000) 2513.
- 2) R. Seguin, A. Schliwa, S. Rodt, K. Pötschke, U. W. Pohl, and D. Bimberg: *Phys. Rev. Lett.* **95** (2005) 257402.
- 3) W. Langbein, P. Borri, U. Woggon, V. Stavarache, D. Reuter, and A. D. Wieck: *Phys. Rev. B* **69** (2004) 161301(R).
- 4) K. Kowalik, O. Krebs, A. Lemaître, S. Laurent, P. Senellart, P. Voisin, and J. A. Gaj: *Appl. Phys. Lett.* **86** (2005) 041907.
- 5) R. M. Stevenson, R. J. Young, P. Atkinson, K. Cooper, D. A. Ritchie, and A. J. Shields: *Nature (London)* **439** (2006) 179.
- 6) S. Seidl, M. Kroner, A. Högele, K. Karrai, R. J. Warburton, A. Badolato, and P. M. Petroff: *Appl. Phys. Lett.* **88** (2006) 203113.
- 7) R. Singh and G. Bester: *Phys. Rev. Lett.* **103** (2009) 063601.
- 8) A. Schliwa, M. Winkelkemper, A. Lochmann, E. Stock, and D. Bimberg: *Phys. Rev. B* **80** (2009) 161307(R).
- 9) A. Mohan, M. Felici, P. Gallo, B. Dwir, A. Rudra, J. Faist, and E. Kapon: *Nat. Photonics* **4** (2010) 302.
- 10) E. Stock, T. Warming, I. Ostapenko, S. Rodt, A. Schliwa, J. A. Töfflinger, A. Lochmann, A. I. Toropov, S. A. Moshchenko, D. V. Dmitriev, V. A. Haisler, and D. Bimberg: *Appl. Phys. Lett.* **96** (2010) 093112.
- 11) T. Noda and T. Mano: *Appl. Surf. Sci.* **254** (2008) 7777.
- 12) N. Koguchi, S. Takahashi, and T. Chikyow: *J. Cryst. Growth* **111** (1991) 688.
- 13) T. Mano, T. Kuroda, S. Sanuginetti, T. Ochiai, T. Tateno, J. S. Kim, T. Noda, M. Kawabe, K. Sakoda, G. Kido, and N. Koguchi: *Nano Lett.* **5** (2005) 425.
- 14) M. Abbarchi, C. A. Mastrandrea, T. Kuroda, T. Mano, K. Sakoda, N. Koguchi, S. Sanguinetti, A. Vinattieri, and M. Gurioli: *Phys. Rev. B* **78** (2008) 125321.
- 15) A. Ohtake: *Surf. Sci. Rep.* **63** (2008) 295.
- 16) T. Belhadj, T. Kuroda, C.-M. Simon, T. Amand, T. Mano, K. Sakoda, N. Koguchi, X. Marie, and B. Urbaszek: *Phys. Rev. B* **78** (2008) 205325.
- 17) T. Kuroda, T. Mano, T. Ochiai, S. Sanguinetti, K. Sakoda, G. Kido, and N. Koguchi: *Phys. Rev. B* **72** (2005) 205301.
- 18) For single QD studies, we prepared a sample with low QD density, where the Ga droplets were formed by supplying 0.043 ML of Ga (0.009 ML/s) at 400°C . The density of QDs was $8.5 \times 10^8 \text{ cm}^{-2}$ as shown in the inset of Fig. 3(a).
- 19) M. Abbarchi, T. Kuroda, T. Mano, K. Sakoda, and M. Gurioli: *Phys. Rev. B* **81** (2010) 35334.
- 20) J. D. Plumhof, V. Křápek, L. Wang, A. Schliwa, D. Bimberg, A. Rastelli, and O. G. Schmidt: *Phys. Rev. B* **81** (2010) 121309(R).